

Synthesis of Poly(styrene) Star Polymers Grown from Sucrose, Glucose, and Cyclodextrin Cores via Living Radical Polymerization Mediated by a Half-Metallocene Iron Carbonyl Complex

Martina H. Stenzel-Rosenbaum, Thomas P. Davis,* Vicki Chen, and Anthony G. Fane

Centre for Advanced Macromolecular Design, School of Chemical Engineering & Industrial Chemistry, The University of New South Wales, Sydney, NSW, Australia 2052

Received December 21, 2000

ABSTRACT: Poly(styrene) stars with 5, 8, and 18 arms were synthesized using living radical polymerization from iodinated glucose, sucrose, and cyclodextrin initiator cores, respectively. The polymerization system comprised of a half-metallocene iron carbonyl complex coupled with titanium(IV) isopropoxide. The reaction kinetics and the molecular weight development were consistent with a living/controlled radical polymerization mechanism. Poly(styrene) stars with a very narrow molecular weight distribution were obtained. Molecular weight analysis by gel permeation chromatography and NMR confirmed that the star structure was consistent with theoretical predictions. The star structure of the polymers was further verified by hydrolysis of the cores to retrieve the polystyrene arms, followed by molecular weight analysis.

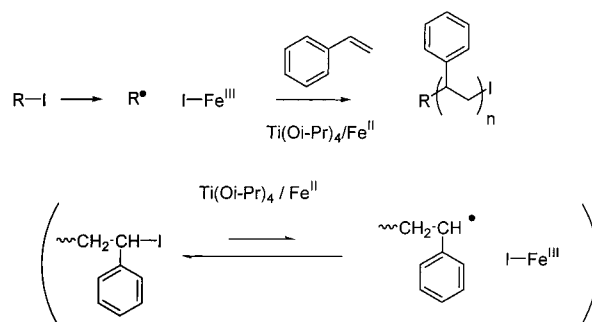
Introduction

In recent years, free radical polymerization has been adopted to synthesize vinyl polymers with pendant saccharide residues.¹ Poly(methyl methacrylate) moieties containing maltoheptose units as side chains have anti-HIV and blood anticoagulant activity.^{2,3} Specific binding of primary hepatocytes to an amphiphilic glycopolymer, poly(*N*-*p*-vinylbenzyl-D-glucuronamide), was investigated by Kim et al.⁴ Kitagawa and Tokiwa⁵ published a very promising route to a fully biodegradable polymer containing sugar moieties via enzymatic synthesis, and Fukuda and co-workers⁶ have adopted atom transfer radical polymerization (ATRP) to graft glycopolymers to a solid surface. Thus, one approach to glycopolymer synthesis is to utilize living radical polymerization⁷ in combination with monomers or initiators that contain sugar residues.

The functionality of sugars can also be utilized as an efficacious route to star polymers. Molecules such as glucose and sucrose have significant advantages as part of a general synthetic strategy as they are cheap, are readily available, and can easily be hydrolyzed using mild conditions to retrieve and assess the polyarms.

A number of initiator/catalyst combinations have been utilized for controlled/living free radical polymerizations in recent years. The most common systems have been based on copper- or ruthenium-mediated polymerization with a wide variety of ligands.^{8–20} More recently, interest has developed in iron-mediated synthesis, and Sawamoto et al.^{21–23} have published the use of half-metallocene iron carbonyl complexes together with iodoester initiators for the living radical polymerization of styrene and acrylates. Louie and Grubbs²⁴ reported highly active iron imidazolylidene catalysts for atom transfer radical polymerization of both styrene and methyl methacrylate. The main advantage of living radical polymerization methods is the ability to create

Scheme 1



well-defined structures in a variety of media with a synthetic route that is tolerant of diverse functionalities. Haddleton and co-workers^{25,26} have described some creative routes to star and oligosaccharide-terminated polymers using copper-mediated ATRP. This approach seems extremely versatile for synthesizing a wide range of functional polymers.

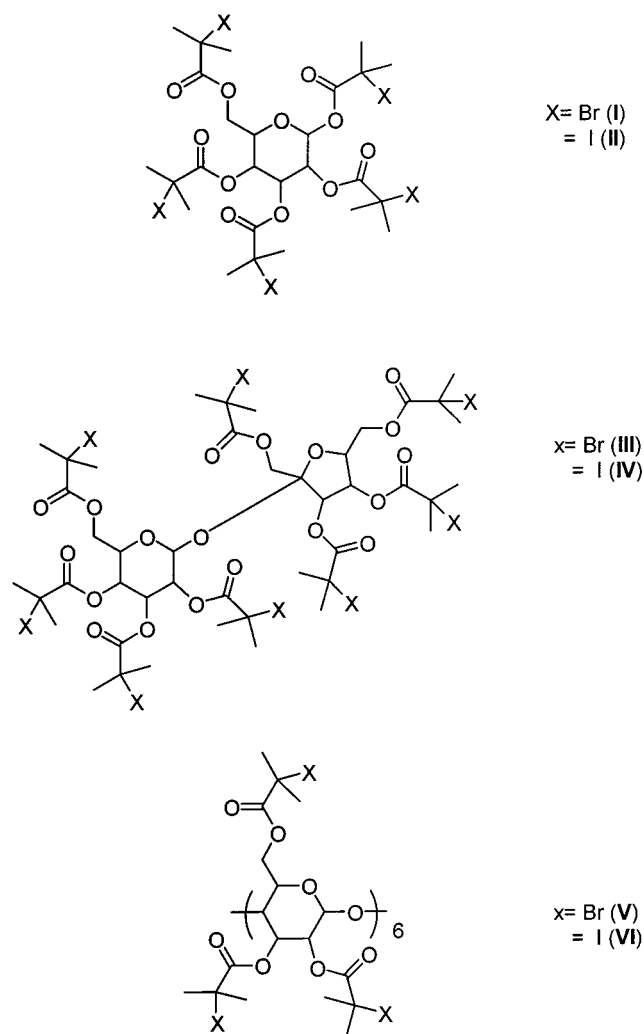
This paper describes work that exploits the iron-mediated approach described by Sawamoto et al.^{21–23} (shown in Scheme 1) using initiators based on iodine-functionalized glucose, sucrose and cyclodextrin cores in a synthetic approach similar to that reported by Haddleton and co-workers in recent conference abstracts.^{27,28} To our knowledge this is the first report of glycopolymer or star synthesis utilizing iron-mediated ATRP.

Experimental Section

Materials. α -D-Glucose (ACS reagent), α -cyclodextrin hydrate, sucrose (98%), 2-bromoisobutyryl bromide, titanium(IV) isopropoxide (97%), and $[\text{FeCp}(\text{CO})_2\text{I}]$ were used as received from Aldrich. Pyridine (ARCOS, ACS reagent), Aceton (Aldrich, 99.5%), and chloroform (99+%, anhydrous) were used without further purification. Styrene (Aldrich, 99%) was purified by elution through a column of activated basic alumina to remove inhibitor. Toluene (99%, Univar) was distilled from potassium hydroxide.

* Correspondence author. Fax 61-2-9385-6250; E mail t.davis@unsw.edu.au.

Chart 1. Star/Core Initiator Structures



Initiator Syntheses. The initiators (Chart 1) were synthesized from glucose, sucrose, and α -cyclodextrin. The iodide functionalization was achieved by utilizing the approach described by Haddleton and co-workers^{25,26} followed by exchange of bromide with iodide in acetone. The direct esterification of sugars with iodoisobutyryl bromide was unsuccessful and led to a crude black mixture.

1,2,3,4,6-Penta-*O*-isobutyryl Bromide- α -D-Glucose (I) (FW 925.09 g/mol) and 1,2,3,4,6-Penta-*O*-isobutyryl Iodide- α -D-Glucose (II) (FW 1160.09 g/mol). 1,2,3,4,6-Penta-*O*-isobutyryl bromide- α -D-glucose (I) was synthesized by the slow addition of 2-bromoisobutyryl bromide (50.0 g, 0.22 mol) to a solution of α -D-glucose (5.0 g, 0.028 mol) in an anhydrous mixture of chloroform (100 mL) and pyridine (50 mL). The solution was refluxed for 3 h while maintaining a dry atmosphere and then stirred at room temperature for a further 12 h. The solution was washed successively with ice cold water, NaOH (0.1 M), and water, prior to drying over anhydrous MgSO_4 . The crude product was recrystallized from methanol to yield white crystals.

Yield: 30%.

¹H NMR (CDCl_3): 1.85–2.04 (m, 30H, $-\text{CH}_3$), 6.42 (d, J = 3.78 Hz, 1H, H-1), 5.25 (dd, J = 3.76 Hz, 9.89 Hz, 1H, H-2), 5.69 (t, J = 9.51 Hz, 1H, H-3), 5.35 (t, J = 9.6 Hz, 1H, H-4), 4.38 (m, 3H, H-5/6).

¹³C NMR (CDCl_3): 30.07–30.73 (CH_3), 55.3–54.4 ($\text{C}(\text{CH}_3)_2$), 89.9 (O–C–O), 68.1–73.0, 163.9–171.5 (C=O).

1,2,3,4,6-Penta-*O*-isobutyryl iodide- α -D-glucose (II) was synthesized by dissolving 1,2,3,4,6-penta-*O*-isobutyryl bromide- α -D-glucose (5.0 g, 5.4 mmol) in dry acetone (50 mL). NaI (5.0 g, 33 mmol) was added and the mixture stirred at room

temperature for 12 h. The solvent was removed and the remaining solid transferred to a separating funnel containing chloroform and a saturated $\text{Na}_2\text{S}_2\text{O}_3$ aqueous solution. The organic layer was dried and the solvent was removed. The crude product was purified by column chromatography using silica gel and an eluent of 2:1 hexane/ethyl acetate.

Yield: 80%.

¹H NMR (CDCl_3): 1.85–2.04 (m, 30H, $-\text{CH}_3$), 6.41 (d, J = 3.78 Hz, 1H, H-1), 5.25 (dd, J = 3.78 Hz, 10.14 Hz, 1H, H-2), 5.69 (t, J = 9.81 Hz, 1H, H-3), 5.33 (t, J = 9.81 Hz, 1H, H-4), 4.38 (m, 3H, H-5/6).

¹³C NMR (CDCl_3): 30.0–31.0 (CH_3), 54.1–55.0 ($\text{C}(\text{CH}_3)_2$), 89.0 (O–C–O), 62.1–69.9, 169.0–171.1 (C=O).

Octa-*O*-isobutyryl Bromide-Sucrose (III) (FW 1520.17 g/mol) and Octa-*O*-isobutyryl Iodide-Sucrose (IV) (FW 1925.23 g/mol). Octa-*O*-isobutyryl bromide-sucrose (III) was synthesized by the slow addition of 2-bromoisobutyryl bromide (50 g, 0.22 mol) to a solution of sucrose (5.0 g, 0.014 mol) in anhydrous pyridine (150 mL). The solution was stirred for 24 h under a dry atmosphere at room temperature. The solution was washed with ice cold water, NaOH (0.1 M), and water, prior to drying over anhydrous MgSO_4 . The crude product was recrystallized from methanol/ H_2O (3:1) to yield white crystals.

Yield: 20%.

¹H NMR (CDCl_3): 1.99 (m, 48H, CH_3), 4.15 (d, 1H, H-5'), 4.46 (m, 5H, H-6'/1'/5), 4.68 (dt, 2H, H-6), 4.81 (d, 1H, H-3'), 5.13 (dd, 1H, H-2), 5.38 (t, 1H, H-4'), 5.67 (t, 1H, H-4), 5.76 (t, 1H, H-3), 5.85 (d, 1H, H-1).

Octa-*O*-isobutyryl iodide-sucrose (IV) was synthesized by dissolving octa-*O*-isobutyryl bromide-sucrose (III) (2.0 g, 1.3 mmol) in dry acetone (20 mL). NaI (3.0 g, 19 mmol) was added and the mixture stirred at room temperature for 12 h. The solvent was removed and the remaining solid transferred to a separating funnel containing chloroform and a saturated $\text{Na}_2\text{S}_2\text{O}_3$ aqueous solution. The organic layer was dried, and the solvent was removed. The crude product was purified by column chromatography using silica gel and an eluent of 2:1 hexane/ethyl acetate.

Yield: 75%.

¹H NMR (CDCl_3): 1.99 (m, 48H, CH_3), 4.15 (d, m, H-5'), 4.44 (m, 5H, H-6'/1'/5), 4.70 (m, 2H, H-6), 4.77 (d, 1H, H-3'), 5.12 (m, 1H, H-2), 5.39 (m, 1H, H-4'), 5.61 (t, 1H, H-4), 5.74 (m, 1H, H-3), 5.85 (d, 1H, H-1).

¹³C NMR (CDCl_3): 30.0–30.7 (CH_3), 54.7–55.5 ($\text{C}(\text{CH}_3)_2$), 88.8 (C1), 102.7 (C2'), 61.5–72.1, 169.0–176.5 (C=O).

Octadeca-*O*-isobutyryl Bromide- α -Cyclodextrine (V) (MW = 3600 g/mol) and Octadeca-*O*-isobutyryl Iodide- α -Cyclodextrine (VI) (MW = 4500 g/mol). Octadeca-*O*-isobutyryl bromide- α -cyclodextrin (V) was synthesized by the slow addition of 2-bromoisobutyryl bromide (50 g, 0.22 mol) to a solution of α -cyclodextrin (5.00 g, 0.005 mol) in anhydrous pyridine (150 mL). The solution was stirred for 24 h under a dry atmosphere at room temperature. The solution was washed with ice cold water, NaOH (0.1 M), and water, respectively, prior to drying over anhydrous MgSO_4 . The crude product was recrystallized from methanol/ H_2O (3:1) to yield white crystals.

Yield: 35%.

¹H NMR (CDCl_3): 1.95 (m, 108H, CH_3), 5.84 (d, 12H, H-1), 4.46 (dd, 6H, H-2), 5.7 (m, 6H, H-3), 5.13/5.38 (t/dd, 6H, H-4), 4.78 (dd, 6H, H-5), 4.45 (m, 6H, H-6).

Octadeca-*O*-isobutyryl iodide- α -cyclodextrine (VI) was synthesized by dissolving octadeca-*O*-isobutyryl bromide- α -cyclodextrine (V) (2.00 g, 0.55 mmol) in dry acetone (20 mL). NaI (3.0 g, 19 mmol) was added and the mixture stirred at room temperature for 12 h. The solvent was removed and the remaining solid transferred to a separating funnel containing chloroform and a saturated $\text{Na}_2\text{S}_2\text{O}_3$ aqueous solution. The organic layer was dried, and the solvent was removed. The crude product was purified by column chromatography using silica gel and an eluent of 2:1 hexane/ethyl acetate.

Yield: 84%.

¹H NMR (CDCl_3): 1.9 (108H, m, CH_3), 6.38 (12H, m, H-1), 5.63 (6H, m, H-3), 5.3 (6H, m, H-4), 5.22 (6H, m, H-5), 4.35 (12H, m, H-2/6).

^{13}C NMR(CDCl_3): 30.0–31.0 (CH_3), 54.1–55.0 ($\text{C}(\text{CH}_3)_2$), 89.0 ($\text{O}-\text{C}-\text{O}$), 62.0–70.0, 169.0–170.5 ($\text{C}=\text{O}$).

Polymerizations. A Schlenk flask was charged with 386 mg of **II** (0.333 mmol), 101 mg of $[\text{FeCp}(\text{CO})_2\text{I}]$ (0.333 mmol), and 950 mg of $[\text{Ti}(\text{O}^i\text{Pr})_4]$ (3.33 mmol) and degassed. Then 30 mL of degassed styrene was added under nitrogen. The homogeneous mixture was additionally degassed by three freeze–pump–thaw cycles and then purged under nitrogen atmosphere. The polymerization was stirred and maintained at 80 °C in an oil bath. After a reaction time of 20 h, a conversion of 21% was obtained. The molecular weight, measured by GPC, is 7600. The polymer was purified by passing through an alumina column and then precipitated in methanol or hexane.

Hydrolysis of Star Polymers. A 100 mg sample of a polystyrene star ($M_n = 22\,000$) was dissolved in a mixture of THF (5 mL), methanol (2 mL), water (0.5 mL), and KOH (150 mg). The mixture was refluxed for 4 days and then precipitated with 1 N HCl. The precipitant polymer was washed with methanol, prior to GPC analyses. Out of the GPC analysis a molecular weight of $M_n = 5500$ for the star arms was obtained.

Analyses. Size Exclusion Chromatography (SEC). SEC analyses were performed on a modular system comprised of the following: a GBC LC1120 HPLC pump operating at room temperature; an in-line ERC-3415 degasser unit; a SIL-10ADVP Shimadzu auto-injector with a stepwise injection control motor with an accuracy of $\pm 1\ \mu\text{L}$; a column set which consisted of a PL 5.0 μm bead size guard column and a set of $3 \times 5.0\ \mu\text{m}$ PL linear columns (10^3 , 10^4 , $10^5\ \text{\AA}$) and a RI detector. Tetrahydrofuran (THF) was utilized as the continuous phase at a flow rate of $1\ \text{mL min}^{-1}$ and a temperature of 40 °C. Polymer solutions were prepared with accurately known concentrations in the range 2–3 mg/mL, while sample injection volumes of 50 μL were used. Lower concentrations were used for the poly(styrene) narrow standards, depending upon their molecular weights.

Conversion. The conversion of the polymerization was measured gravimetrically.

NMR Compositional Analysis. ^1H NMR spectra were recorded on a 300 MHz (Bruker ACF300) spectrometer using CDCl_3 (Aldrich) as solvent.

Results and Discussion

Stars Derived from a Glucose Core (II). The catalyst system developed by Kotani et al.^{21–23} utilizes a titanium alkoxide ($\text{Ti}(\text{O}^i\text{Pr})_4$) as an additive, as shown in Scheme 1. Our initial experiments used the iron complex and the titanium alkoxide in the same proportion ($[\text{II}]:[\text{FeCp}(\text{CO})_2\text{I}]:[\text{Ti}(\text{O}^i\text{Pr})_4] = 1:1:10$), but altered the concentration of toluene. The polymerization experiments were all held at 80 °C. Several first-order kinetic plots are shown in Figure 1 and indicate that the individual radical concentrations were constant throughout each polymerization. The pseudo-first-order rate constants (k_{obs}) and the derived radical concentrations are tabulated in Table 1. The low radical concentration favors living behavior.

In the early stages of the polymerizations, some induction times and slower rates are observed. The cause of this is unknown and it is difficult to ascertain whether this was observed previously by Kotani and co-workers.^{21–23} It may be a genuine feature of the reaction, or it may be caused by some impurity. However, at higher conversions, a steady-state rate is observed and the polymerizations show excellent living characteristics. Some curvature in the rate plot is expected, as the chain propagation rate has been shown to be chain length dependent. Olaj et al.²⁹ have shown that a ~20% decrease in k_p occurs extending over several hundreds of degrees of polymerization. In star polymer

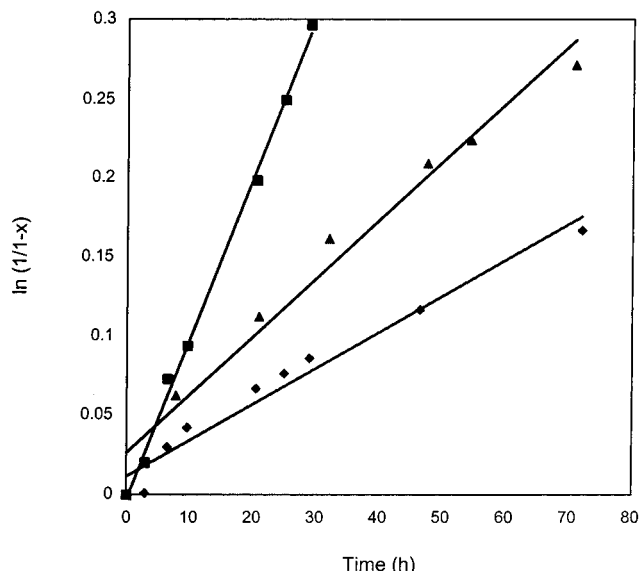


Figure 1. Pseudo-first-order plots of the polymerization of styrene at 80 °C with varying toluene concentrations ($[\text{styrene}]$, **II**, $[\text{FeCpI}(\text{CO})_2]$, $[\text{Ti}(\text{O}^i\text{Pr})_4]$ in mM: (\blacklozenge) [3000], [5], [5], [50]; (\blacktriangle) [6000], [10], [10], [100]; (\blacksquare) [bulk], [15], [15], [150]). X represents the conversion.

Table 1. Radical Concentration Calculated from the Pseudo First-Order Kinetic Plot (k_{obs}) and k_p of Styrene at Different Temperature

experiment: [styrene], [II], $[\text{FeCpI}(\text{CO})_2]$, $[\text{Ti}(\text{O}^i\text{Pr})_4]$ in mM, (temp in °C)	k_{obs} (1/s)	k_p (L/mol s)	$[\text{R}^\cdot]$ (mol/L)
[3000], [5], [5], [50], (80)	6.33×10^{-7}	660	9.59×10^{-10}
[6000], [10], [10], [100], (80)	9.16×10^{-7}	660	1.38×10^{-9}
[bulk], [15], [15], [150], (80)	2.80×10^{-6}	660	4.24×10^{-9}
[6000], [10], [10], [100], (60)	4.42×10^{-7}	386	1.14×10^{-9}
[6000], [10], [10], [100], (100)	4.37×10^{-6}	1195	3.65×10^{-9}

synthesis, this effect may be expected to extend over a much larger chain length.

At any given conversion, the molecular weight and polydispersity are unaffected by the concentrations of styrene, initiator or catalyst provided they are kept in the same ratio. This is shown clearly in Figure 2. Typical GPC chromatograms are given in Figure 3 depicting narrow, unimodal peaks indicating no evidence for star–star coupling by termination events. Strong evidence for the absence of significant termination is the decreasing polydispersity index over the observed conversion range, shown in Figure 2. Extremely narrow polydispersities have been reported by Sawamoto^{21–23} using this polymerization system. Sawamoto et al. optimized their developed system and achieved polydispersities down to 1.06 and narrow unimodal GPC peaks up to high conversions with absence of shoulders at higher molecular weight. Our results confirm the efficacy of this particular synthetic method.

The molecular weight of the star polymers measured by GPC is less than the expected calculated values. This is attributed to the different hydrodynamic volumes of the star molecules when compared with the linear polystyrene standards. As a result, the GPC presumably underestimates the actual molecular weight. Previous publications have suggested the use of NMR to estimate the molecular weight of star polymers. Kotani et al.²² used the signal arising from the proton adjacent to the iodide end group ($\delta = 4.19\ \text{ppm}$) to determine the

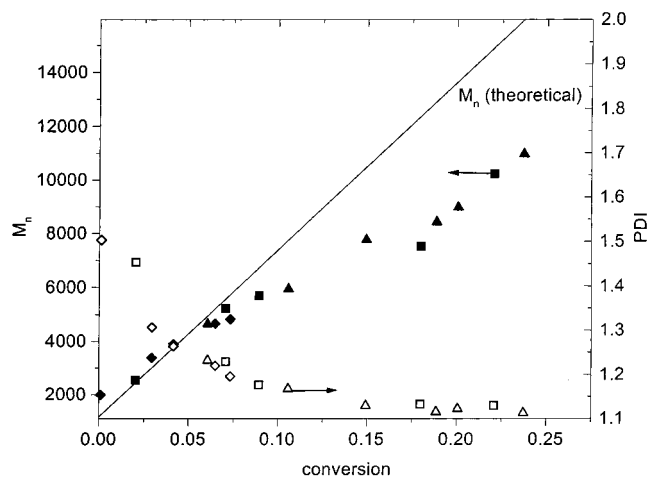


Figure 2. Effect of dilution on molecular weight with constant monomer, initiator and catalyst ratios on molecular weight (solid dots) and polydispersity (open dots) ([styrene], [II], [Fe(Cp)I(CO)₂], [Ti(O'Pr)₄] in mM: (◆) [3000], [5], [5], [50]; (▲) [6000], [10], [10], [100]; (■) [bulk], [15], [15], [150]). The open symbols represent the polydispersity values. (—) calculated molecular weight

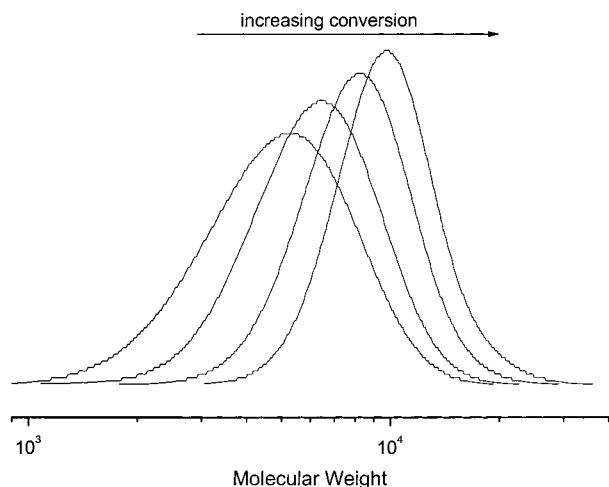


Figure 3. GPC traces of polystyrene stars formed by polymerization with initiator core II ([styrene] = 6 M, [II] = 10 mM, [Fe(Cp)I(CO)₂] = 10 mM, [Ti(O'Pr)₄] = 100 mM) after 8 (6% conversion), 21 (11%), 32 (15%), and 71 h (24%).

molecular weight of the linear polystyrene and compare to the GPC results. Unfortunately, this particular signal is obscured by proton signals derived from the glucose core. Consequently, the methyl groups of the initiator were used, which shift from $\delta = 1.9$ to $\delta = 0.85$ ppm after adding styrene (Figure 4). Despite the errors arising from this procedure, an estimation of the true molecular weight can be made. The data shown in Table 2, clearly indicate that the molecular weight measurements obtained from NMR data concur with the calculated (predicted) values. This supports the underestimation of the GPC procedure of the actual molecular weights that do in fact conform with calculated values, supporting the living nature of the polymerization reaction.

The effect of temperature on the star syntheses is shown in Figure 5. As expected, the reaction rate increases with temperature. Unfortunately, the rate increase is accompanied by some loss of control as indicated by an increase in the polydispersity index from 1.12 (60 °C) to 1.22 (100 °C) at 20% conversion. The

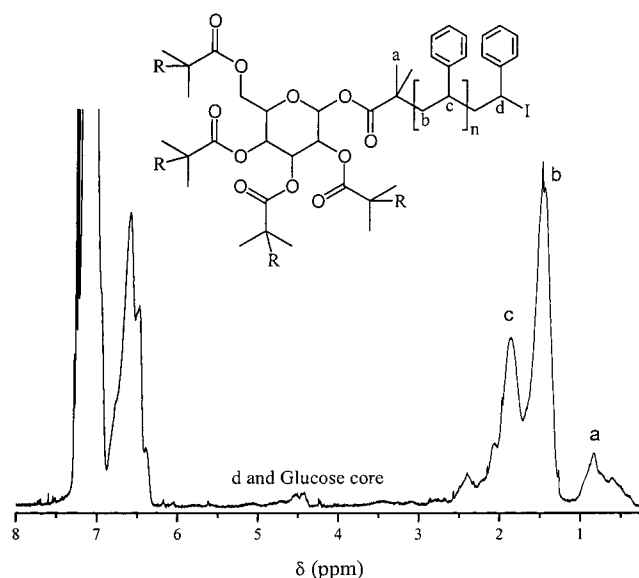


Figure 4. NMR spectrum of glucose-based polystyrene star in CDCl₃. (The protons labeled e were used in the molecular weight calculation.)

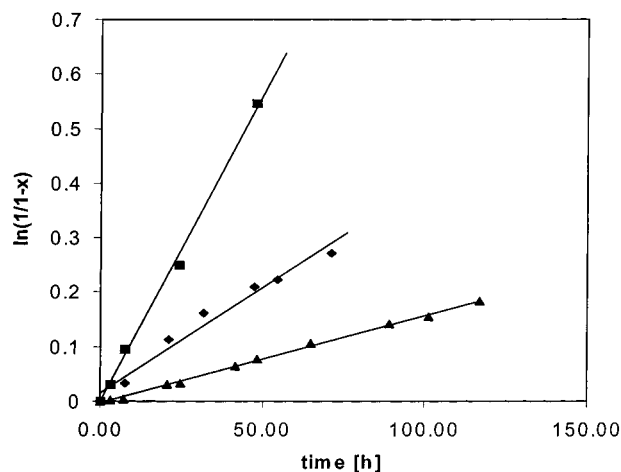


Figure 5. Effect of temperature [(■) 100 °C, (◆) 80 °C, (▲) 60 °C] on rate of polymerization ([styrene], [II], [Fe(Cp)I(CO)₂], [Ti(O'Pr)₄] in mM = [6000], [10], [10], [100]).

Table 2. Comparisons of Calculated ATRP Molecular Weights with Values Derived from GPC and NMR ([styrene], [II], [Fe(Cp)I(CO)₂], [Ti(O'Pr)₄] = [6000], [10], [10], [100], 80 °C)

% convn	$M_n(\text{GPC}) \times 10^{-3}$	$M_n(\text{predicted}) \times 10^{-3}$	$M_n(\text{NMR}) \times 10^{-3}$
6	4.65	4.95	4.30
11	5.90	7.80	8.10
15	7.80	10.5	12.1
19	8.40	12.9	12.3
20	9.00	13.7	12.5
24	11.0	16.0	16.2

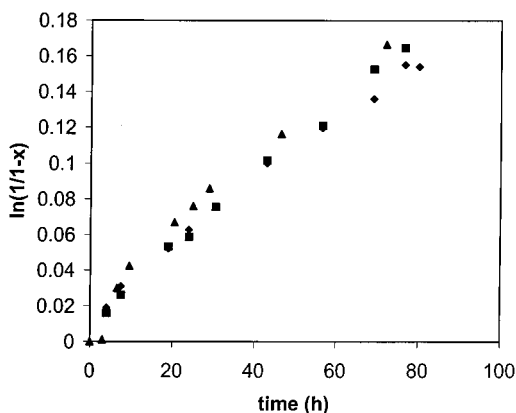
pseudo-first-order rate constants and the radical concentrations for these experiments are given in Table 1. The calculated radical concentration is found to increase with increasing temperature.

The role of the Fe(II) and titanium complex was also subjected to some analysis (Table 3). Experiments with the glucose-based initiator confirm the previous findings of Kotani et al.²² that an increase in the concentration of the iron complex has negligible effect on the conversion, but a detrimental influence on the polydispersity index. This may be attributed to the existence of higher

Table 3. Effect of the Concentration of $\text{Ti}(\text{O}^i\text{Pr})_4$ on Star Polydispersity^a

$[\text{Ti}(\text{O}^i\text{Pr})_4]$ (mM)	% convn	$M_n \times 10^{-4}$	PDI
10	9	1.38	1.46
100	10	1.72	1.30
10	42	2.62	1.40
100	41	2.86	1.21

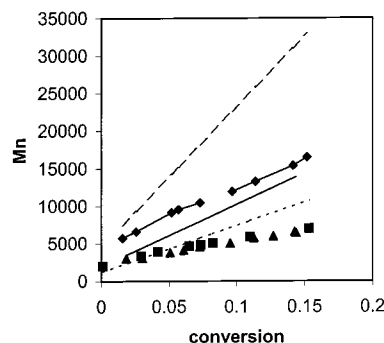
^a ([styrene], [II], $[\text{Fe}(\text{Cp})\text{I}(\text{CO})_2]$, $[\text{Ti}(\text{O}^i\text{Pr})_4]$ = [6000], [10], [10], [100 or 10], 100 °C).

**Figure 6.** Rate of reaction with glucose- (▲), sucrose- (◆), and α -cyclodextrin- (■) based initiators ([styrene], [iodide-groups], $[\text{Fe}(\text{Cp})\text{I}(\text{CO})_2]$, $[\text{Ti}(\text{O}^i\text{Pr})_4]$ = [3000], [25], [5], [50], 80 °C). X represents the conversion.

radical concentrations of propagating radicals resulting in excessive termination and star–star coupling. The titanium alkoxide has a positive influence on the polydispersity index as shown in Table 3. Kotani et al. found the polymerization to be the uncontrolled in the absence of $\text{Ti}(\text{O}^i\text{Pr})_4$.²² The precise role of the $\text{Ti}(\text{O}^i\text{Pr})_4$ is unknown although the cyclic voltammetry results of Kotani et al.²³ indicate the existence of a coordination compound between titanium and the $\text{Fe}(\text{II})$ complex enhancing the oxidation–reduction process by lowering the oxidation and reduction potential.

Sucrose- (IV) and Cyclodextrin- (VI) Based Initiators. Initiators with higher functionality were also prepared based on sucrose (8 arms) and cyclodextrin (18 arms). These were then employed for the polymerization of styrene in toluene. The concentration of iodide was maintained at a constant level in order to afford a direct comparison. The following polymerization conditions were set: styrene (6 M), iodide groups (25 mM), $\text{Fe}(\text{Cp})\text{I}(\text{CO})_2$ (10 mM), and $\text{Ti}(\text{O}^i\text{Pr})_4$ (50 mM). Using these reaction conditions several kinetic experiments were performed. The pseudo-first-order kinetic plots are shown in Figure 6. All three initiating systems exhibit similar behavior.

Therefore, regardless of the functionality of the initiator, the branch length should be identical in each case. Figure 7 shows the molecular weights measured by GPC. Deviations from the theoretical expectation can be attributed to changes in the hydrodynamic volume of the molecules. This originates from the molecular structure, viz., changes in the branching structure, and for the case of cyclodextrin, the core itself is a major constituent of the polymer. Therefore, this molecule can be viewed as a hybrid structure. Consequently, the deviation is most significant for the 18-arm star. As expected, the polydispersity of the stars decreases with the number of branches. The glucose-based star (five branches) has a PDI of 1.15 at 20% conversion, whereas

**Figure 7.** Conversion vs theoretical M_n and the GPC found molecular weights of polystyrene stars based on glucose (▲), sucrose (◆), and α -cyclodextrin (●) ([styrene], [iodide groups], $[\text{Fe}(\text{Cp})\text{I}(\text{CO})_2]$, $[\text{Ti}(\text{O}^i\text{Pr})_4]$ = [3000], [25], [5], [50], 80 °C). Star/core initiator structures.**Table 4.** Molecular Weight of Polystyrene Stars from GPC (Calibration with Linear Polystyrene) Compared to the Theoretical (Expected) Molecular Weight and the Molecular Weight of Single Branches after Isolation from the Core

$M_n(\text{GPC})$ of stars with linear styrene calibration $\times 10^{-3}$	core	$M_n(\text{theoretical}) \times 10^{-3}$	$M_n(\text{GPC})$ of arms $\times 10^{-3}$	no. of arms
2.70	IV	6.15	0.68	8
3.40	IV	11.3	1.08	8
3.85	IV	13.8	1.35	8
22.0	II	32.0	5.50	5
5.00	II	6.30	1.00	5

the cyclodextrin star has a PDI of 1.08 at an equivalent conversion. This conforms to the Flory equation where $M_w/M_n(\text{PDI}) = 1 + (1/f)$, where f is the functionality of the core.

Hydrolysis of Star Polymers. For further evidence of the star structure and confirmation of the molecular weight several of the glucose- and sucrose-derived star polymers were hydrolyzed to recover the arms for analyses. The disconnection of core and arms leads to linear polystyrene arms, which can now be analyzed with GPC using a linear polystyrene calibration. The molecular weight results are shown in Table 4. The results (accounting for experimental errors) confirm the presumed structure of the stars. The molecular weight of the stars, calculated from the arm length and the number of arms, is now close to the expected molecular weight. This supports the explanation that the GPC underestimates the real molecular weight because of the change of the hydrodynamic volume, which becomes more and more significant with increasing number of arms.

Conclusions

The iron-mediated radical polymerization reaction originally described by Kotani et al.^{21–23} furnishes excellent control over styrene polymerizations. Well-defined star polymers were synthesized using sucrose, glucose, and cyclodextrin cores. In concurrent research, we have also used copper-based ATRP reactions, and in comparison, the iron system generally resulted in narrower molecular weight distributions. However, the restriction to iodine-based initiators in the iron system is a significant drawback, as this adds an additional step to the initiator synthesis, and iodide polymer end groups can be rather unstable. The requirement for a metal alkoxide cocatalyst is also a disadvantage, as the polymerization has a high sensitivity toward humidity

or protic impurities (decomposition of the Ti complex) and oxygen (oxidation of the iron complex). Despite these problems, the synthetic approach utilizing iron has attractions. Kotani et al.^{21–23} have suggested the advantages of cost and low toxicity. In this regard the recent publication by Louie and Grubbs²⁴ is exciting as it shows the potential for improved iron-based systems.

Acknowledgment. We wish to thank Professor David Haddleton for providing us with prepublication manuscripts and data. We gratefully acknowledge a DAAD (German Academic Exchange Service) Scholarship (HSPIII) for M.H.S.-R.

References and Notes

- (1) Miyata, T.; Nakamae, K. *Trends Polym. Sci.* **1997**, *5*, 198.
- (2) Hashimoto, K.; Ohsawa, R.; Imai, N.; Okada, M. *J. Polym. Sci., Part A: Polym. Chem.* **1999**, *37*, 303.
- (3) Yoshida, T.; Akasaka, T.; Choi, Y.; Hattori, K.; Yu, B.; Mimura, T.; Kaneko, Y.; Nakashima, H.; Aragaki, E.; Premanathan, M.; Yamamoto, N.; Uryu, T. *J. Polym. Sci., Part A: Polym. Chem.* **1999**, *37*, 789.
- (4) Kim, S. H.; Goto, M.; Cho, C. S.; Akaike, T. *Biotech. Lett.* **2000**, *22*, 1049.
- (5) Kitagawa, M.; Tokiwa, Y. *Kobunshi Ronbunshu* **2000**, *57*, 629.
- (6) Ejaz, M.; Ohno, K.; Tsujii, Y.; Fukuda, T. *Macromolecules* **2000**, *33*, 2870.
- (7) For a discussion on the controversy of appropriate terminology, see: Darling, T. R.; Davis, T. P.; Fryd, M.; Gridnev, A. A.; Haddleton, D. M.; Ittel, S. D.; Matheson, R. R.; Moad, G.; Rizzardo, E. *J. Polym. Sci., Part A: Polym. Chem.* **2000**, *38*, 1706.
- (8) Haddleton, D. M.; Shooter, A. J.; Heming, A. M.; Crossman, M. C.; Duncalf, D. J.; Morsley, S. R. In *Controlled Radical Polymerization*; Matyjaszewski, K., Ed.; ACS Symposium Series 685; American Chemical Society: Washington, DC, 1998; p 284.
- (9) Haddleton, D. M.; Heming, A. M.; Kukulj, D.; Duncalf, D. J.; Shooter, A. J. *Macromolecules* **1998**, *31*, 2016.
- (10) Haddleton, D. M.; Waterson, C.; Derrick, P. J.; Jasieczek, C. B.; Shooter, A. J. *Chem. Commun.* **1997**, 683.
- (11) Haddleton, D. M.; Jasieczek, C. B.; Hannon, M. J.; Shooter, A. J. *Macromolecules* **1997**, *30*, 2190.
- (12) Kato, M.; Kamigaito, M.; Sawamoto, M.; Hiashimura, T. *Macromolecules* **1995**, *28*, 1721.
- (13) Matyjaszewski, K. *Macromolecules* **1998**, *31*, 4710.
- (14) Matyjaszewski, K. In *Controlled Radical Polymerization*; Matyjaszewski, K., Ed.; ACS Symposium Series 685; American Chemical Society: Washington, DC, 1998; p 258.
- (15) Nishikawa, T.; Ando, T.; Kamigaito, M.; Sawamoto, M. *Macromolecules* **1997**, *30*, 2244.
- (16) Percec, V.; Barboiu, B. *Macromolecules* **1995**, *28*, 7970.
- (17) Percec, V.; Barboiu, B.; Neumann, A.; Ronda, J. C.; Zhao, M. *Macromolecules* **1996**, *29*, 3665.
- (18) Wang, J.-S.; Matyjaszewski, K. *Macromolecules* **1995**, *28*, 7572.
- (19) Wang, J.-S.; Matyjaszewski, K. *J. Am. Chem. Soc.* **1995**, *117*, 5614.
- (20) Wang, J.-S.; Matyjaszewski, K. *Macromolecules* **1995**, *28*, 7901.
- (21) Kotani, Y.; Kamigaito, M.; Sawamoto, M. *Macromolecules* **2000**, *33*, 6746.
- (22) Kotani, Y.; Kamigaito, M.; Sawamoto, M. *Macromolecules* **1999**, *32*, 6877.
- (23) Kotani, Y.; Kamigaito, M.; Sawamoto, M. *Macromolecules* **2000**, *33*, 3543.
- (24) Louie, J.; Grubbs, R. H. *Chem. Commun.* **2000**, 1479.
- (25) Haddleton, D. M.; Edmonds, R.; Heming, A. M.; Kelly, E. J.; Kukulj, D. *New J. Chem.* **1999**, *23*, 477.
- (26) Haddleton, D. M.; Ohno, K. *Biomacromolecules* **2000**, *1*, 152.
- (27) Ohno, K.; Haddleton, D. M.; Kukulj, D.; Wong, B. *Am. Chem. Soc. Polym. Prepr.* **2000**, *41* (1), 478.
- (28) Edmonds, R.; Haddleton, D. M.; Bon, S. A. F. *Am. Chem. Soc. Polym. Prepr.* **2000**, *41* (1), 444.
- (29) Olaj, O. F.; Vana, P.; Zoder, M.; Kornherr, A.; Zifferer, G.; *Macromol. Rapid Commun.* **2000**, *21*, 913.

MA0021803